Development of an adaptive tuned vibration absorber with magnetorheological elastomer

2006 Smart Mater. Struct. 15 N111

(http://iopscience.iop.org/0964-1726/15/5/N02)

INSTITUTE OF PHYSICS PUBLISHING SMART MATERIALS AND STRUCTURES
Smart Mater. Struct. **15** (2006) N111–N116 doi:10.1088/0964-1726/15/5/N02

TECHNICAL NOTE

Development of an adaptive tuned vibration absorber with magnetorheological elastomer

Hua-xia Deng, Xing-long Gong[1] and Lian-hua Wang

CAS Key Laboratory of Mechanical Behavior and Design of Materials, Department of Mechanics and Mechanical Engineering, University of Science and Technology of China, Hefei 230027, People's Republic of China

E-mail: gongxl@ustc.edu.cn

Received 21 February 2006, in final form 11 July 2006
Published 9 August 2006
Online at stacks.iop.org/SMS/15/N111

Abstract
In this technical note we develop an adaptive tuned vibration absorber (ATVA) based on the unique characteristics of magnetorheological elastomers (MREs), whose modulus can be controlled by an applied magnetic field. The MRE used in the developed ATVA was prepared by curing a mixture of 704 silicon rubber, carbonyl iron particles and a small amount of silicone oil under a magnetic field. The ATVA works in shear mode and consists of an oscillator, smart spring elements with MREs, a magnet conductor and two coils. Natural frequencies of the ATVA under different magnetic fields were both theoretically analyzed and experimentally evaluated by employing a beam structure with two ends supported. The experimental results demonstrated that the natural frequency of the ATVA can be tuned from 55 to 82 Hz. The relative frequency change is as high as 147%. Furthermore, the absorption capacity of the developed ATVA can achieve as high as 60 dB, which was also experimentally justified.

(Some figures in this article are in colour only in the electronic version)

1. Introduction

Magnetorheological (MR) materials are smart materials which have MR effects and many unique properties under magnetic fields. The MR effects are that the rheological properties will be changed under an applied magnetic field. Since their discovery by Rabinow in 1948 [1], MR materials have developed into a family with MR fluids, MR foams and MR elastomers [2]. The most common MR material is MR fluids (MRFs), which are magnetically polarizable particles suspended in viscous fluids [3]. The general criterion to estimate the MR effect of MRFs is the variation capability of dynamic yield stresses within a post-yield regime under an applied magnetic field. Numerous applications based on MRFs benefit from the properties that the dynamic yield stress can be continuously, rapidly and reversibly controlled by the applied magnetic field. Such applications have been applied to a variety of fields, such as in the automotive industry [4–6], earthquake resistance [7] and vibration control [8] and have found commercialization and industrialization. For instance, the LORD Corporation of American has been professionally researching, manufacturing, and distributing MRFs based devices, such as brakes, clutches and variable-friction dampers. But MRFs also exhibit some shortcomings, such as deposition, environmental contamination [9] and sealing problems, which hinder their wide application.

MR elastomers (MREs), the structural solid analogues of MRFs, may be a good solution to overcome these disadvantages. MREs are composed of polarizable particles dispersed in a polymer medium. Typically, magnetic fields are

[1] Author to whom any correspondence should be addressed.

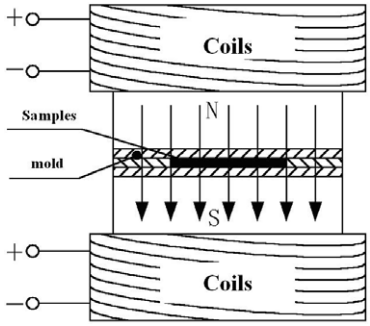

Figure 1. Schematic diagram of the fabrication method.

Figure 2. Photograph of the modified DMA.

applied to the polymer composite during crosslinking so that particles form chainlike or columnar structures, which are fixed in the matrix after curing [10]. The difference between MREs and MRFs is that the MR effect of MREs is the field-dependent modulus within the pre-yield regime [11]. Such properties indicate that MREs are promising for many applications, such as adaptive tuned vibration absorbers (TVAs), stiffness tunable mounts and suspensions, and variable impedance surfaces. Relative to MRFs, the application of MREs is still at an exploratory stage. Watson [12] filed a patent for using MREs, "Method and apparatus for varying the stiffness of a suspension bushing"; Ginder and coworkers [13, 14] constructed and tested tunable automotive mounts and bushings based on MR elastomers which could be applied to minimize the effect of suspension resonances excited by torque variation due to worn brake rotors by shifting the resonance away from the excitation frequency. They also did pioneering work on the development of an adaptive tunable vibration absorber (ATVA) using MREs [15]. Their initial experimental results indicated that the ATVA had the capability to shift frequency from 500 to 610 Hz.

Other smart materials could also be applied to develop ATVAs. A traditional dynamic vibration absorber (DVA) theoretically brings the object base to rest at a single excitation frequency, the resonance frequency of the DVA. It means that the absorber is usually used to suppress a single harmonic excitation of the vibrating systems. For many practical systems, which have complex vibration sources or wide vibration frequency bandwidth, the passive absorber will lose its effect and potentially aggravate the base vibration. Williams and co-workers [16, 17] did a lot of work on ATVA with shape memory alloys (SMA), which can vary its frequency by changing environmental temperature. Davis *et al* [18, 19] applied a piezoceramic inertial actuator (PIA) to ATVA which could vary the natural frequency from 243 to 257 Hz. Magnetostrictive material was used by Flatau *et al* [20] to develop an ATVA achieving a natural frequency variation from 1400 Hz to over 2000 Hz through application of DC magnetic fields.

The aim of this project is to investigate the application of MREs to vibration controls. To this end, a shear mode vibration absorber working with MREs was developed. Both theoretical analysis and experimental testing were carried out to investigate both its frequency-shift property and vibration absorption capacity.

2. MRE materials

2.1. Material preparation

The MRE materials consist of a 704 silicone rubber which was provided by Wuxi Xida adhesive factory as a matrix, carbonyl iron particles (70% mass ratio) from BASF with a size of 3–5 μm, and a small amount of silicone oil provided by Hangzhou West Lake organic silicon factory. A schematic diagram of the fabrication method is shown in figure 1. In the first step of the fabricating process, all ingredients are thoroughly blended with an agitator. Then the mixture is packed into an aluminum mold and placed in the vacuum to remove the air in the mixture. After that, the mold is sealed and placed in a magnetic field of 1 T for 24 h. The particles will be arranged in chain formation due to the anisotropic magnetic forces among the particles. When the elastomer is cured, such ordered structure is locked in the matrix. The experimental results reveal that MREs with chains of iron particles have good MR effects.

2.2. MRE characterization

Figure 2 shows a photograph of the MRE testing system, which is modified by our group on the base of the Dynamic Mechanical Analyzer (DMA) system from the Triton Co. (model: tritec2000). To measure MRE properties under various magnetic fields, an electromagnet was developed, which can provide a magnetic field intensity up to 1100 mT. With this system, both the shear modulus and the loss factor against magnetic field at various excitation frequencies were measured. The results are shown in figure 3. It can be seen from figure 3(a) that the shear modulus shows an increasing trend with magnetic field intensity. However, the increasing slope decreases with the increment of magnetic field, which is due to magnetic saturation. In addition, the modulus also shows an increasing trend with loading frequency, which justifies that MRE exhibits viscoelastic behavior. Figure 3(b) shows that the loss factor is independent of magnetic field and frequency, as demonstrated previously [10].

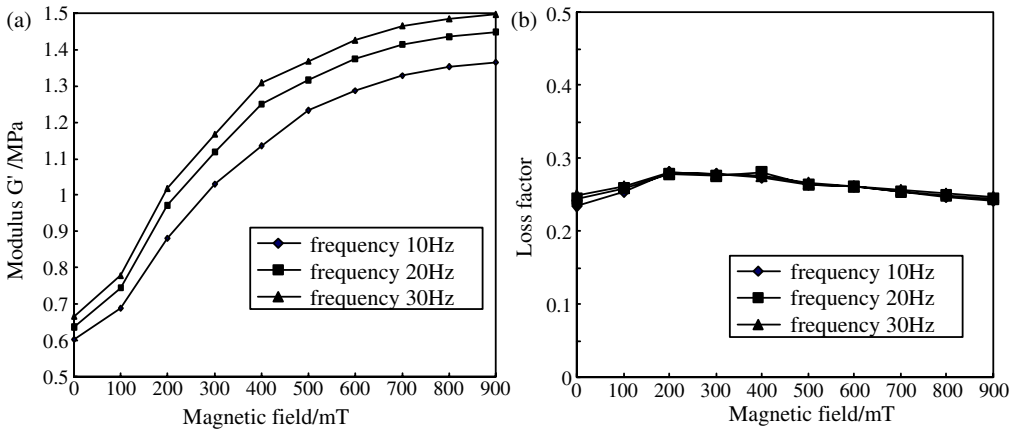

Figure 3. Variation of shear modulus and loss factor with magnetic field at different loading frequencies.

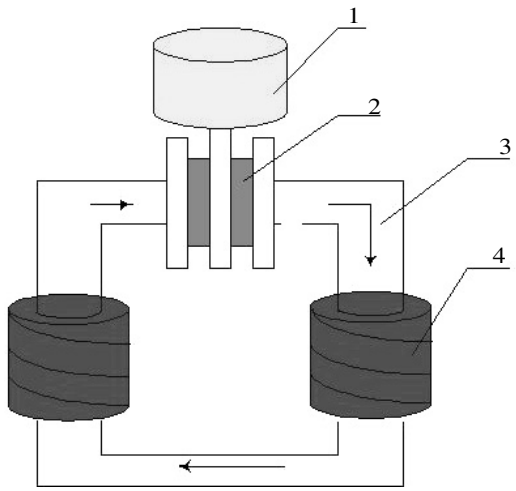

Figure 4. Schematic diagram of the ATVA developed 1: Oscillator; 2: MREs; 3: Magnetic conductor; 4: Coils.

Figure 5. Photograph of the ATVA developed.

3. ATVA with MRE

3.1. ATVA structure

A schematic diagram of the ATVA developed is shown in figure 4. As shown in this figure, the ATVA consists of four main parts: oscillator, smart spring element with MREs, magnetic conductor, and coils. The system forms into a closed C-shape electromagnet (see photograph in figure 5). The working principle of the system is as follows. The magnetic field is created by two coils and the field strength is controlled by the coil current, provided by an external DC power. As MRE's shear modulus depends on the field strength, the equivalent stiffness of the ATVA changes with the field strength as well as the coil current. Consequently, the natural frequency of the ATVA can be controlled by the coil current. Thus, the ATVA natural frequency can be changed by tuning the coil current to trace the external excitation frequency. When the tuned ATVA frequency matches the excitation frequency, the vibration can be attenuated significantly. This point will be theoretically addressed in the following section.

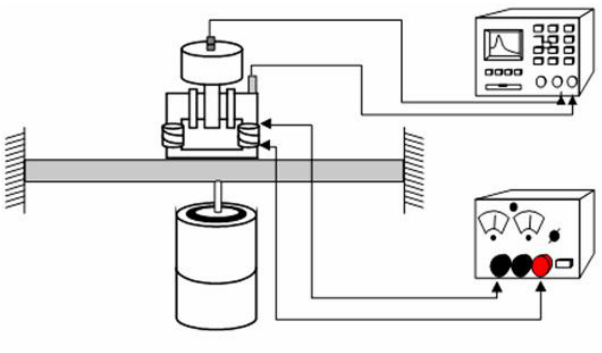

Figure 6. The system for evaluation of the frequency-shift property.

3.2. Experimental study of frequency-shift property

For simplicity, a beam with both ends supported is used to investigate the frequency-shift capability of the MREs. The experimental setup is shown in figure 6. The beam is made up of low carbon steel, with a size of 930 mm × 100 mm × 11 mm.

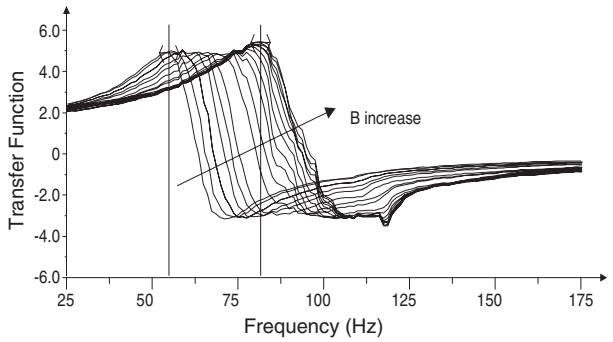

Figure 7. The transfer function versus frequency at various magnetic fields.

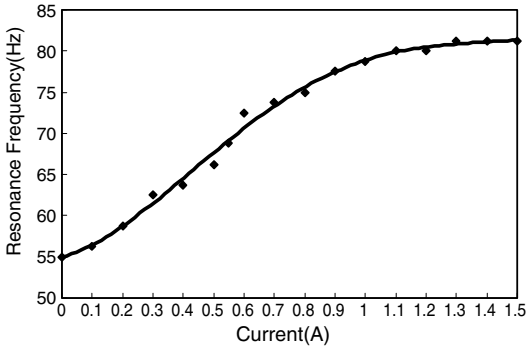

Figure 8. The relationship between applied current and resonance frequency.

The material parameters are: Young's modulus $E = 200$ GPa, density $\rho = 7800$ kg m^{-3}, Poisson's ratio $\nu = 0.3$, and the loss factor $\eta = 0.05$. Using modal analysis, its first and second mode natural frequencies are 64 Hz and 250 Hz, respectively. As shown in figure 6, the experimental procedure is as follows. The ATVA developed is placed at the center of the beam. White noise excitation applied to the beam is generated by an exciter (model: JZK-10, manufactured by Sinocera Piezotronics Inc., China). Two accelerometers (model: PCB 3510A) are placed on the oscillator and the base beam to measure their responses, respectively. The measured signals are sent to the dynamic signal analyzer (model: Signal Calc ACE DP240, Data Physics Corp.). The transfer function can be obtained by using FFT analysis. The frequency-shift capability at various magnetic fields of the ATVA based on MREs is shown in figure 7. It shows that the curve of transfer function moves rightward with the increase in the magnetic field. The resonance frequency can be obtained by reading the peak-to-peak value. By tuning the coil current, the relationship of the resonance frequency of the absorber versus the coil current can be obtained and it is shown in figure 8. The resonance frequency increases from 55 Hz at 0 A to 81.25 Hz at 1.5 A. Its relative frequency change is as high as 147%, which agrees well with the theoretical result using the MRE's testing data.

3.3. Theoretical analysis of the frequency-shift property

The resonance frequency of the TVA is represented as

$$f = \frac{1}{2\pi}\sqrt{\frac{k_\tau}{m}} \tag{1}$$

where m is the mass of the oscillator, and k_τ is the equivalent shear stiffness.

In the shear direction, k_τ is given by

$$K_\tau = \frac{GA}{h} \tag{2}$$

where G is MRE's shear modulus, A is the shear area, and h is the thickness of MREs.

The MRE shear modulus G consists of two terms, as below

$$G = G_0 + \Delta G_\mathrm{d} \tag{3}$$

where G_0 is the initial natural frequency without any magnetic field, and ΔG_d is the shear modulus increment under the applied magnetic field. The double pole model is widely used to predict the magnetic induced shear modulus increment [21]. Using this model, the shear modulus increment under the magnetic field is given by [22]

$$\Delta G_\mathrm{d} = 36\phi\mu_\mathrm{f}\mu_0\beta^2 H_0^2\left(\frac{R}{d}\right)^3\zeta \tag{4}$$

where $\beta = (\mu_\mathrm{p} - \mu_\mathrm{f})/(\mu_\mathrm{p} + 2\mu_\mathrm{f}) \approx 1$, μ_0 is the vacuum permeability, $\mu_\mathrm{p} \approx 1000$ and $\mu_\mathrm{f} \approx 1$ are the relative permeability of the particles and silicon rubber matrix, respectively. ϕ is volume fraction, R is the average particle radius, d is the particle distance before deflection, H_0 is the applied magnetic field intensity, and $\zeta = \sum_{k=1}^{\infty} 1/k^3 \approx 1.202$. When the magnetic field is high enough, some particles will saturate, equation (4) is no longer valid. When all particles saturate, equation (4) will be replaced as

$$\Delta G_\mathrm{d} = 4\phi\mu_\mathrm{f}\mu_0 M_\mathrm{s}^2\left(\frac{R}{d}\right)^3 \tag{5}$$

where M_s is the saturation intensity of the particles.

Substituting equations (2) and (3) into equation (1), the natural frequency is rewritten as

$$f = f_0 + \Delta f \tag{6}$$

where f_0 is the resonant frequency without magnetic field, and Δf is the shift of resonance frequency due to the applied magnetic field.

$$f_0 = \frac{1}{2\pi}\sqrt{\frac{G_0 A}{mh}} \tag{7}$$

$$\Delta f = \frac{1}{2\pi}\sqrt{\frac{G_0 \times A}{m \times h}}\left(\sqrt{1 + \frac{\Delta G_\mathrm{d}}{G_0}} - 1\right). \tag{8}$$

From equation (7), the initial resonant frequency of the ATVA can be designed to match the vibration system, the focus of the vibration attenuation. Equation (8) reveals that the frequency-shift capacity is not only proportional with the MR effect but also relative to the initial shear modulus. The larger initial modulus with the same MR effect will cause the wider frequency-shift bandwidth. When $\Delta G_\mathrm{d} \ll G_0$, equation (8) can be approximately substituted by equation (9)

$$\Delta f = \frac{\Delta G_\mathrm{d}}{4\pi}\sqrt{\frac{A}{G_0 mh}}. \tag{9}$$

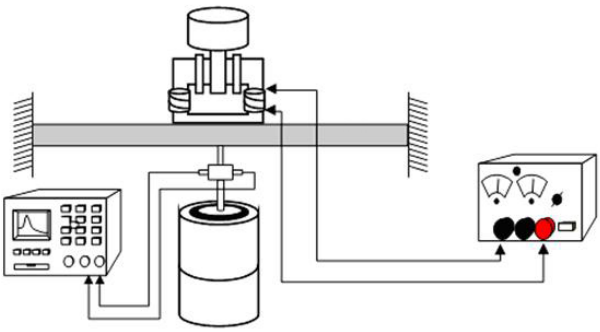

Figure 9. The evaluation system for vibration attenuation.

The frequency shift is proportional to the shear modulus increases, and it can be seen from the beginning of the curve shown in figure 8.

When ΔG_d is as large as G_0, equation (8) is not valid. Substituting equation (4) into (7), the frequency-shift can be rewritten as below

$$\Delta f = \frac{1}{2\pi}\sqrt{\frac{G_0 \times A}{m \times h}}\left(\sqrt{1+\frac{36\phi\mu_f\mu_0\beta^2 H_0^2\left(\frac{R}{d}\right)^3\zeta}{G_0}}-1\right). \tag{10}$$

Similarly, substituting equation (5) into (7), the frequency shift at saturation status is a constant as given by

$$\Delta f = \frac{1}{2\pi}\sqrt{\frac{G_0 \times A}{m \times h}}\left(\sqrt{1+\frac{4\phi\mu_f\mu_0 M_s^2\left(\frac{R}{d}\right)^3}{G_0}}-1\right). \tag{11}$$

The theoretical trend presented by equations (9)–(11) agrees well with the results shown in figure 8 qualitatively.

3.4. The study on vibration attenuation

The effect of vibration absorption can be evaluated by the system shown in figure 9. Compared with the frequency-shift experiment, the major difference is that an impedance head is induced. As shown in this figure, the impedance head connects with the beam and the exciter. The exciter provides a sinusoidal excitation to the beam with a linear frequency scan from low to high. The natural frequency will be tuned by changing the coil current to trace the excitation frequency. The base point impedance with various magnetic fields can be measured by the dynamic signal analyzer. If the magnetic field is fixed, the absorber can be considered as a classical passive TVA with fixed resonance frequency. To evaluate the vibration absorption capacity, a ratio γ of base point admittance with TVA and without TVA is used.

The system in figure 9 can be simplified as shown in figure 10. Suppose the force and velocity applied to the base point O is F_0, and V_0, respectively. The resultant forces and velocities at the lower and upper points of the static mass M_s are F_s^b, V_s^b and F_s^t, V_s^t, respectively. The resultant force and velocity of the absorber mass M_A are F_A and V_A. The admittance at point O is defined as H_0^b and given by

$$H_0^b = \frac{V_0}{F_0} = \frac{j\omega}{M_B}\sum_{k=1}^{n}\frac{\Phi_k^2(x_0)}{\omega_k^2(1+j\eta)-\omega^2} \tag{12}$$

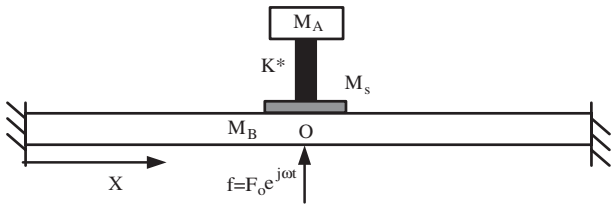

Figure 10. Simplified model of the evaluation system.

where ω_k and ϕ_k are the kth natural frequency and mode function, x_0 is the coordinator of the point O, n is the mode number, η is the loss factor, ω is the excitation frequency, $j = \sqrt{1}$. Equation (11) can be simplified as

$$V_0 = \frac{\Delta H}{H_0^b + \Delta H}H_0^b F_0,$$
$$\Delta H = 1\Big/\left(j\omega M_s + \frac{j\omega M_A K^*}{K^* - \omega^2 M_A}\right) \tag{13}$$

where ΔH is the additional admittance at the point O due to the absorber and the mass, K^* is the complex stiffness of the absorber. The complex stiffness can be expressed by conventional spring's stiffness K, damping factor C and damping ratio ξ:

$$K^* = K(1 + j\omega C/K) = K(1 + 2j\omega\omega_0\xi M_A/K). \tag{14}$$

The admittance at the point O with the absorber is given by

$$H_A = \frac{\Delta H}{H_0^b + \Delta H}H_0^b. \tag{15}$$

When there is no active mass, the admittance at the point O is given by

$$H_0 = \frac{\Delta H^s}{H_0^b + \Delta H^s}H_0^b, \qquad \Delta H^s = 1/(j\omega M_s). \tag{16}$$

The ratio γ to reflect the effect of vibration absorption capacity can be defined as

$$\gamma = 20(|H_A/H_O|). \tag{17}$$

The comparison of vibration absorption capacity between the adaptive TVA and the passive one is shown in figure 11, where the upper data are the results of passive TVA whose resonance frequency is fixed at 64 Hz (the first natural frequency of the beam) and the lower data are the results of ATVA whose frequency is tuned to trace the excitation frequency. As shown in figure 11, the experimental data and numerical curve are very close. It indicates that the dynamic model is reasonable and the experimental data is reliable. For the passive TVA, the best vibration attenuation efficiency occurs at the antiresonance frequency. The effect become worse sharply while the excitation frequency is apart from beam sympathetic frequency and a new resonance hump occurs at 37 Hz. For ATVA, limited to the MR effect of the spring element, ATVA cannot be experimentally evaluated at the whole frequency band. In the tunable frequency band, the comparison between adaptive TVA and the passive one indicates that ATVA has

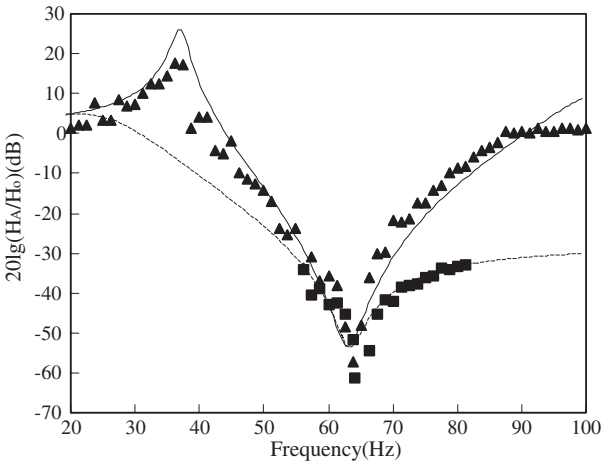

Figure 11. The vibration attenuation of absorbers ■ adaptive (experimental data); ▲ passive (experimental data); - - - - adaptive (numerical data); —— passive (numerical data).

better absorbing effects than the passive TVA. For example, at 81 Hz, the ATVA's effect of vibration absorption is −33 dB, while it is −8 dB for the passive TVA. For even wider bandwidth, theoretical analysis predicts that the ATVA also has better effects and there is no resonance hump at the formant frequency of the passive TVA.

4. Conclusion

A shear mode ATVA with MRE was developed in this paper. It consists of an oscillator, coils, a magnetic conductor and smart spring elements with MREs. Both theoretical and experimental results indicate that the resonance frequency of the developed ATVA can be controlled by electrical currents. The resonance frequency varies from 55 Hz at 0 A to 81.25 Hz at 1.5 A. Its relative frequency change is as high as 147%. To evaluate the vibration absorption capability of TVA, a beam with two ends supported is used as an object base and the ratio γ of base point admittance with TVA and without TVA is used. The experimental results agree well with the theoretical calculation and they all demonstrate that the ATVA developed has better performance than a conventional passive absorber in terms of its frequency-shift property and vibration absorption capacity.

Acknowledgments

The authors want to thank Professor P Q Zhang, H L Sun, Y S Zhu, J F Li, Z B Xu for their support and especially thank Dr X Z Zhang for useful discussion and Dr W H Li (University of Wollongong of Australia) for his help with English revision. This work is supported by the BRJH Project of the Chinese Academy of Sciences and SRFDP of China (No 20050358010).

References

[1] Rabinow J 1948 The magnetic fluid clutch *AIEE Trans.* **67** 1308–15
[2] David Carlson J and Jolly M R 2000 MR fluid, foam and elastomer devices *Mechatronics* **10** 555–69
[3] Zhang X Z, Gong X L, Zhang P Q and Wang Q M 2004 Research on mechanism of squeeze-strengthen effect in magnetorheological fluids *J. Appl. Phys.* **96** 2359–64
[4] Li W H and Du H 2003 Design and experimental evaluation of a magnetorheological brake *Int. J. Adv. Manuf. Technol.* **21–27** 508–15
[5] Ginder J M 1998 Behavior of magnetorheological fluids *MRS Bull.* **23–28** 26–9
[6] Ginder J M, Davis L C and Elie L D 1996 Rheology of magnetorheological fluids: models and measurements *Int. J. Mod. Phys.* B **10** 3293–303
[7] Dyke S J, Spencer B F, Sain M K and Carlson J D 1998 An experimental study of MR dampers for seismic protection *Smart Mater. Struct.* **7** 693–703
[8] Jung H J, Spencer B F and Lee I W 2003 Control of seismically excited cable-stayed bridge employing magnetorheological fluid dampers *J. Struct. Eng.* **129** 873–83
[9] Shen Y, Golnarghi M F and Heppler G R 2004 Experimental research and modeling of magnetorheological elastomers *J. Intell. Mater. Syst. Struct.* **15** 27–35
[10] Gong X L, Zhang X Z and Zhang P Q 2005 Fabrication and characterization of isotropic magnetorheological elastomers *Polym. Testing* **24–25** 669–76
[11] Zhou G Y 2003 Shear properties of a magnetorheological elastomer *Smart Mater. Struct.* **12** 139–46
[12] Watson J R 1997 Method and apparatus for varying the stiffness of a suspension bushing *US Patent Specification* 5,609,353
[13] Stewart W M, Ginder J M, Elie L D and Nichols M E 1998 Method and apparatus for reducing brake shudder *US Patent Specification* 5,816,587
[14] Ginder J M *et al* 2000 Controllable-stiffness components based on magnetorheological elastomers *Proc. SPIE* **3985** 418–25
[15] Ginder J M, Schlotter W F and Nichols M E 2001 Magnetorheological elastomers in tunable vibration absorbers *Proc. SPIE* **4331** 103–10
[16] Williams K A, Chiu G T-C and Bernhard R J 1999 Passive–adaptive vibration absorbers using shape memory alloys *Proc. SPIE* **3668** 630–64
[17] Williams K A, Chiu G T-C and Bernhard R J 2005 Dynamic modeling of a shape memory alloy adaptive tuned vibration absorber *J. Sound Vib.* **280** 211–34
[18] Davis C L, Lesieutre G A and Dosch J 1995 A tunable electrically shunted piezoceramic vibration absorber *Proc. SPIE* **3045** 51–9
[19] Davis C L and Lesieutre G A 2000 An actively tuned solid-state vibration absorber using capacitive shunting of piezoelectric stiffness *J. Sound Vib.* **3** 601–17
[20] Flatau A B, Dapino M J and Calkins F T 1998 High band width tenability in a smart vibration absorber *Proc. SPIE* **3327** 463–73
[21] Shiga T, Okada A and Kurauchi T 1995 Magnet-roviscoelastic behavior of composite gels *J. Appl. Polym. Sci.* **58** 787–92
[22] Davis L C 1999 Model of magnetorheological elastomers *J. Appl. Phys.* **85** 3348–51